Geomechanics and Engineering, *Vol. 39, No. 3 (2024) 257-271*
https://doi.org/10.12989/gae.2024.39.3.257

Dynamic analysis of viscoelastic porous functionally graded plates resting on elastic foundation

Ömer Faruk Çapar[1], Mehmet Halil Çalım[2], Mehmet Bugra Özbey[1] and Yavuz Cetin Cuma*[1]

[1]*Department of Civil Engineering, Adana Alparslan Turkes Science and Technology University, Türkiye*
[2]*Department of Civil Engineering, Çukurova University, Adana, Türkiye*

(*Received February 27, 2023, Revised September 6, 2024, Accepted October 22, 2024*)

Abstract. In this study, free and forced vibration behaviour of viscoelastic porous functionally graded (VPFG) plates resting on elastic foundations are investigated. Differential equations are obtained via higher order shear deformation theory. Equations of motion are obtained through energy formulations and Hamilton's principle. Navier's method based on double Fourier series is employed for the solution. Damping effect is implemented into the analysis by means of Kelvin and linear standard viscoelastic models. Viscoelastic material properties are used instead of elastic properties by means of the correspondence principle. Displacements of the plates are determined in Laplace domain and transformed into time domain by using Durbin's Modified Inverse Laplace transform method. The proposed algorithm's accuracy is validated through free and damped vibration analyses on VPFG plate, with results compared to existing studies in the literature. The study examines the influence of viscoelastic damping parameters, porosity volume fraction indexes, foundation characteristics, porosity distribution patterns and material property variations on the damped forced vibration response.

Keywords: forced vibration; free vibration; linear viscoelastic models; porous functionally graded plates

1. Introduction

Plates have countless applications in many engineering fields such as; aerospace, mechanical, civil, etc. Plates may be required to have different properties in the same application, i.e., tiles on space shuttles need to endure extreme heat on the outside while having sufficient ductility on the inside. Additionally, these elements are subjected to dynamic loads. Therefore, investigation of the dynamic behaviour of functionally graded plates is crucial. There are numerous studies available on the free and forced vibration of plates.

Free and forced vibration analysis of rectangular plates have been investigated by using Ritz method (Leissa 1973, Nagino *et al.* 2008, Choe *et al.* 2018), Navier's solution method (Reddy 2000, Matsunaga 2008, Thai and Choi 2012, Mantari *et al.* 2014, Akavci 2014, Akavci and Tanrıkulu 2015, Sayyad and Ghugal 2015, Arefi and Meskini 2019, Vinh and Huy 2021, Dogan 2022), finite element methods (FEM) (Bardell 1991, Reddy 2000, Pandit *et al.* 2007, Ramu and Mohanty 2012, , Xuan *et al.* 2012, Dogan 2022, Burlayenko *et al.* 2015, Tabatabaei and Fattahi 2022, Vinh *et al.* 2022), Galerkin Method (Shahsavari *et al.* 2018). Effect of various shear deformation theories (Cho *et al.* 1991, Reddy 2000, Vel and Batra 2004, Sobhy 2013, Nedri *et al.* 2014, Akavci and Tanrıkulu 2015, Shao *et al.* 2017), boundary conditions (Leissa 1973, Bardel 1991, Nagino *et al.* 2008, Baferani *et al.* 2011, Messina 2011, Thai and Choi 2012, Xuan *et al.* 2012, Sobhy 2013, Sayyad and Ghugal 2015, Burlayenko *et al.* 2015, Kumar *et al.* 2018, Xue *et al.* 2019, Tabatabaei and Fattahi 2022, Vinh *et al.* 2022, Alavi *et al.*. 2022, Zhang *et al.* 2020), power law coefficient (Matsunaga 2008, Xuan *et al.* 2012, Thai and Choi 2012, Kumar *et al.* 2018, Zhang *et al.* 2020, Dogan 2022) and plate geometries (Nagino *et al.* 2008, Choe *et al.* 2018, Xue *et al.* 2019, Arefi and Meskini 2019, Zhang *et al.* 2020), material type (Xuan *et al.* 2012, Mantari *et al.* 2014, Rad *et al.* 2017, Choe *et al.* 2018), plate thickness (Pandit *et al.* 2007, Thai and Choi 2012, Ramu and Mohanty 2012), ground conditions (Akavci 2014, Shahsavari *et al.* 2018, Vinh and Huy 2021) are taken into consideration. Various materials are used in analysis such as: porous functionally graded (PFG) (Shahsavari *et al.* 2018, Zhao *et al.* 2018, Arefi and Meskini 2019, Zhang *et al.* 2020, Vinh and Huy 2021, Alnujaie *et al.* 2021, Alavi *et al.* 2022), exponentially graded material (EGM) (Shahsavari *et al.* 2018, Rabhi *et al.* 2020), functionally graded material (FGM) (Reddy 2000, Vel and Batra 2004, Matsunaga 2008, Baferani *et al.* 2011, Thai and Choi 2012, Neves *et al.* 2012, Xuan *et al.* 2012, Mantari *et al.* 2014, Akavci 2014, Akavci and Tanrıkulu 2015, Rad *et al.* 2017, Benahmed *et al.* 2017, Choe *et al.* 2018, Kumar *et al.* 2018, Boulefrakh *et al.* 2019, Rachedi *et al.* 2020, Chikr *et al.* 2020, Dogan 2022, Tabatabaei and Fattahi 2022), isotropic (Nagino *et al.* 2008), bi-directional functionally graded (BFG) (Vinh *et al.* 2022), laminated composite (Cho *et al.* 1991, Pandit *et al.* 2007, Messina 2011, Nedri *et al.* 2014, Sayyad and Ghugal 2015, Shao *et al.* 2017), composite (Burlayenko *et al.* 2015, Nebab *et al.* 2020).

Reddy (2000) performed forced vibration analysis of functionally graded plates by using both Navier's method

*Corresponding author, Ph.D.
E-mail: cumayc@atu.edu.tr

ISSN: 2005-307X (Print), 2092-6219 (Online)

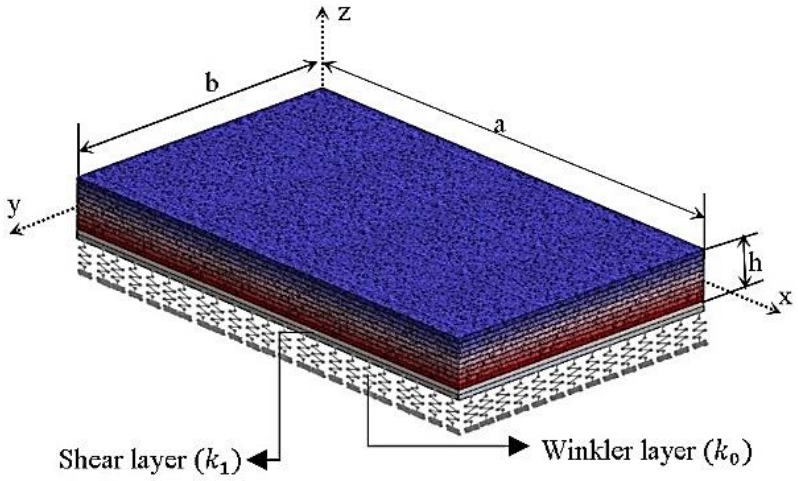

Fig. 1 PFG plate resting on elastic foundation

and finite element model. Akavci (2014) carried out the free vibration analysis for functionally graded plates resting on elastic foundation by using higher order shear deformation theory. They obtained the closed form solution by implementing Navier's method. Dogan (2022) examined dynamic behaviours of viscoelastic functionally graded plates under impulsive loads.

Material compositions were considered as perfect in most of the previous studies. Occurrence of porosities in the fabrication process is inevitable. Therefore, investigating the effect of porosity on the dynamic behaviour proposes to be a crucial aspect. Recently, studies considering porosities in the material have been published.

Shahsavari *et al.* (2018) observed the effect of three elastic foundation models and three porosity distributions on the free vibration behaviour of PFG plates resting on elastic foundation. Trigonometric shear deformation theory in displacement field and Galerkin method for solution of the eigenvalue problem were used in their study.

Functionally graded materials (FGMs) are composed of a combination of metals and ceramics, leveraging the heat and corrosion resistance of ceramics along with the high tensile strength of metals. They are particularly advantageous in applications like space shuttle tiles, where ductility is required on the interior and extreme temperature resistance on the exterior. Moreover, FGMs offer a significant advantage over traditional laminated composites by reducing the risk of delamination failure. The material properties in FGMs continuously vary, eliminating interfaces between different materials and thus preventing material discontinuities that could lead to delamination. However, the production process of these materials is not flawless, often resulting in the formation of pores. Reflecting porosity in dynamic analyses is therefore crucial. Additionally, porous materials are widely used in aerospace engineering due to their lightweight nature and hold a significant place in the literature. In the analysis of plates and shells, linear elastic material models are often assumed for simplicity. Although this assumption facilitates the analysis, adopting a viscoelastic material model provides more realistic results due to the internal friction within the materials. Consequently, many studies focus on viscoelastic materials, with the Kelvin viscoelastic model and the linear standard model being among the most popular. Given these factors, investigating the dynamic behaviour of porous functionally graded viscoelastic plates is of great importance. However, there is a gap in the literature concerning the dynamic analysis of functionally graded viscoelastic plates supported by an elastic foundation. Best to the authors' knowledge, the transient response of viscoelastic functionally graded rectangular plates with porosities resting on elastic foundation is investigated for the first time in the present study. Displacement field of rectangular plates are determined by using the higher order shear deformation theory (HSDT). By using energy method and Hamilton's principle simultaneously, equations of motion are derived. Using the energy method and Navier's solution stiffness and mass matrices are obtained. Comparison studies for free vibration on PFG plates and forced vibration of FGM plates are done. Finally, a parametric study considering the damped forced vibration of PFG plates on elastic foundation is carried out. Obtained results are given in graphical form.

2. Formulation

Functionally graded plates are used in many engineering applications. Multiple materials are combined for the purpose of utilizing their effective features in order to fabricate stronger structures. The dynamic behaviour of these composite materials has been a popular subject. Frequently, material composition consists of a ceramic and a metal. Although, many of the preceding studies consider the material to be perfectly fabricated, porosities will occur during manufacturing process. In Fig. 1 an PFG plate composed of ceramic and metal with porosities is shown.

Two types of Porosity Distributions (PD) are implemented in this study. First type (PD-I) represents the evenly spread porosities and second type (PD-II) represents

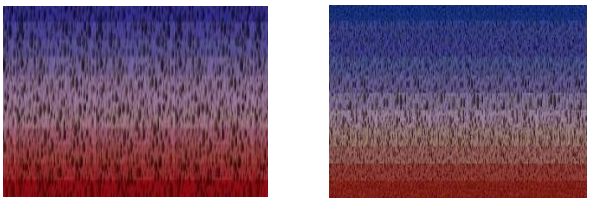

PD-I PD-II

Fig. 2 Porosity distributions

the symmetrically spread porosities. According to the modified mixture rule, material properties through thickness "$P(z)$" (Young's modulus E, mass density ρ and Poisson's ratio ν) of the rectangular plate for *PD-I* and *PD-II* are defined by Shahsavari *et al.* (2018) as

$$P(z) = P_m + (P_c - P_m)\left(\frac{1}{2} + \frac{z}{h}\right)^p - (P_c - P_m)\frac{\xi}{2} PD - I \quad (1)$$

$$P(z) = P_m + (P_c - P_m)\left(\frac{1}{2} + \frac{z}{h}\right)^p - (P_c - P_m)\frac{\xi}{2}\left(1 - \frac{2|z|}{h}\right) PD - II \quad (2)$$

P_c and P_m denotes the material properties of ceramic and metal, respectively. h is plate thickness, ξ is porosity volume fraction index, p is power-law exponent.

Displacement field regarding the HSDT is expressed as the function of Cartesian coordinates (x, y, z) and time (t). The displacements u, v and w are presented (Akavci 2014)

$$u(x,y,z,t) = u_o(x,y,t) - z\,\frac{\partial w_o}{\partial x} + f(z)\,\theta_x(x,y,t) \quad (3)$$

$$v(x,y,z,t) = v_o(x,y,t) - z\,\frac{\partial w_o}{\partial y} + f(z)\,\theta_y(x,y,t) \quad (1)$$

$$w(x,y,z,t) = w_o(x,y,t) \quad (5)$$

u_o, v_o and w_o are the displacements at the mid-plane of the plate and θ_x and θ_y are rotations of section normal with respect to x and y axis. $f(z)$ is the shape function of the transverse shear strain and stress distributions along the thickness direction. In this study a trigonometric shape function is used given by Akavci (2014).

$$f(z) = Tan(h)\left(\frac{z\,r}{h}\right) - \left(\frac{z\,r}{h}\right) Sech^2\left(\frac{r}{2}\right) \quad (6)$$

"r" is a numerical parameter used in calculation $f(z)$. Optimum value of this parameter is determined as 3 by Akavci (2014). Normal and shear strains can be obtained via the linear elasticity theory using the mid-plane deformations.

$$\varepsilon_x = \frac{\partial u}{\partial x} = \frac{\partial u_0}{\partial x} - z\frac{\partial^2 w_0}{\partial x^2} + f(z)\frac{\partial \theta_x}{\partial x} \quad (7)$$

$$\varepsilon_y = \frac{\partial v}{\partial y} = \frac{\partial v_0}{\partial y} - z\frac{\partial^2 w_0}{\partial y^2} + f(z)\frac{\partial \theta_y}{\partial y}$$

$$\gamma_{yz} = \frac{\partial v}{\partial z} + \frac{\partial w}{\partial y} = \frac{\partial f(z)}{\partial z}\theta_y$$

$$\gamma_{xz} = \frac{\partial u}{\partial z} + \frac{\partial w}{\partial x} = \frac{\partial f(z)}{\partial z}\theta_x$$

$$\gamma_{xy} = \frac{\partial u}{\partial y} + \frac{\partial v}{\partial x} = \frac{\partial u_0}{\partial y} + \frac{\partial v_0}{\partial x} + f(z)\frac{\partial \theta_x}{\partial y} + f(z)\frac{\partial \theta_y}{\partial x} - 2z\frac{\partial^2 w_0}{\partial x \partial y}$$

Displacements are considerably small in comparison to the thickness of the plate. Therefore, strain (ε_z) and stress (σ_z) in z direction are taken zero. The transition from strain $(\varepsilon_x, \varepsilon_y, \gamma_{yz}, \gamma_{xz}, \tau_{xy})$ to stress $(\sigma_x, \sigma_y, \tau_{yz}, \tau_{xz}, \tau_{xy})$ for the rectangular plate can be expressed with the help of the following function (Cuma *et al.* 2023).

$$\begin{bmatrix}\sigma_x\\ \sigma_y\\ \tau_{yz}\\ \tau_{xz}\\ \tau_{xy}\end{bmatrix} = \begin{bmatrix}Q_{11} & Q_{12} & 0 & 0 & 0\\ Q_{21} & Q_{22} & 0 & 0 & 0\\ 0 & 0 & Q_{44} & 0 & 0\\ 0 & 0 & 0 & Q_{55} & 0\\ 0 & 0 & 0 & 0 & Q_{66}\end{bmatrix}\begin{bmatrix}\varepsilon_x\\ \varepsilon_y\\ \gamma_{yz}\\ \gamma_{xz}\\ \gamma_{xy}\end{bmatrix} \quad (8)$$

where Q_{ij} denote the stiffness terms of the plate which are

$$Q_{11} = Q_{22} = \frac{E(z)}{(1-\nu^2)} \quad (9)$$

$$Q_{12} = Q_{21} = \frac{\nu E(z)}{(1-\nu^2)}$$

$$Q_{44} = Q_{55} = Q_{66} = \frac{E(z)}{2(1+\nu)}$$

Derivation of the equations of motion relevant to the displacement field and constitutive equations can be obtained by using the Hamilton's principle which can be stated as

$$\int_{t_1}^{t_2} (\delta U - \delta T + \delta V_e) dt = 0 \quad (10)$$

where δ denotes variation, U represents strain energy and is expressed as

$$U = \int_v \left(\sigma_{xx}\varepsilon_{xx} + \sigma_{yy}\varepsilon_{yy} + \tau_{xy}\gamma_{xy} + \tau_{xz}\gamma_{xz} + \tau_{yz}\gamma_{yz}\right) dV \quad (11)$$

T is kinetic energy which is obtained by the Eq. (12)

$$T = \frac{1}{2}\int_v \rho(z)(\dot{u}^2 + \dot{v}^2 + \dot{w}^2)\, dV \quad (12)$$

here $\rho(z)$ and $(\dot{})$ are mass density and derivative over time (t), respectively. V_e denotes the potential energy of the elastic foundation and is obtained as

$$V_e = \frac{1}{2}\int_A \left[k_o w^2 + k_1\left\{\left(\frac{dw}{dx}\right)^2 + \left(\frac{dw}{dy}\right)^2\right\}\right] dA \quad (13)$$

k_o and k_1 in the formulation represent Winkler stiffness and the shear stiffness of the elastic foundation, respectively. Substituting the expressions in Eqs. (11)-(13) into Eq. (10), the following expression is obtained.

$$\int_{t_1}^{t_2}\left(\begin{array}{c}\int_V [\sigma_x\,\delta\varepsilon_x + \sigma_y\delta\varepsilon_y + \tau_{xy}\delta\gamma_{xy} + \tau_{xz}\delta\gamma_{xz} + \tau_{yz}\delta\gamma_{yz}\\ -\rho(z)(-\ddot{u}\delta u - \ddot{v}\delta v - \ddot{w}\delta w)]dv\\ +\int_A [k_o w\delta w - k_1(w_{,xx}\delta w + w_{,yy}\delta w)]dA\end{array}\right) dt = 0 \quad (14)$$

Interaction between the force, moment and stress components along with moment of inertia and mass density are given in Eq. (15).

$$\{N_x, N_y, N_{xy}\} = \int_{-h/2}^{h/2} \{\sigma_x, \sigma_y, \tau_{xy}\}\, dz \quad (15)$$

$$\{Q_x, Q_y, Q_{xy}\} = \int_{-h/2}^{h/2} f(z)\{\sigma_x, \sigma_y, \tau_{xy}\}\, dz$$
$$\{M_x, M_y, M_{xy}\} = \int_{-h/2}^{h/2} \{\sigma_x, \sigma_y, \tau_{xy}\}\, z\, dz$$
$$\{R_x, R_y\} = \int_{-h/2}^{h/2} f'(z)\,\{\tau_{xz}, \tau_{yz}\}\, dz$$
$$\{I_1, I_2, I_3, I_4, I_5, I_6\} = \int_{-h/2}^{h/2} \rho(z)\{1, z, z^2, f(z), zf(z), f(z)^2\}\, dz$$

By using the relations between stress-strain-force-moment and mass moment of inertia given in Eqs. (7), (8), (15), the expressions in Eq. (14) can be reorganized in terms of the coefficients of δu_0, $\delta v_0, \delta w_0$, $\delta\theta_x$ and $\delta\theta_y$ leading to the derivation of the motion's equations for plates resting on elastic foundation.

$$-N_{x,x} - N_{xy,y} + I_1\ddot{u}_o - I_2\ddot{w}_{o,x} + I_4\ddot{\theta}_x = 0 \tag{16}$$
$$-N_{y,y} - N_{xy,x} + I_1\ddot{v}_o - I_2\ddot{w}_{o,y} + I_4\ddot{\theta}_y = 0$$
$$-M_{x,xx} - M_{y,yy} - 2M_{xy,y,x} + I_1\ddot{w}_o + I_2\left(\ddot{u}_{o,x} + \ddot{v}_{o,y}\right) - I_3\left(\ddot{w}_{o,xx} + \ddot{w}_{o,yy}\right) + I_5\left(\ddot{\theta}_{y,y} + \ddot{\theta}_{x,x}\right) + k_0\, w_0 - k_1\left(w_{0,xx} + w_{0,yy}\right) = 0$$
$$-Q_{x,x} - Q_{xy,y} + R_x + I_4\ddot{u}_o - I_5\ddot{w}_{o,x} + I_6\ddot{\theta}_x = 0$$
$$-Q_{y,y} - Q_{xy,x} + R_y + I_4\ddot{v}_o - I_5\ddot{w}_{o,y} + I_6\ddot{\theta}_y = 0$$

Force and moment components in the equations of motion can be determined by substituting Eqs. (7) and (8) into Eq. (15).

$$N_x = A_{11}u_{o,x} + A_{12}v_{o,y} - B_{11}w_{o,xx} - B_{12}w_{o,yy} + C_{11}\theta_{x,x} + C_{12}\theta_{y,y} \tag{17}$$
$$N_y = A_{21}u_{o,x} + A_{22}v_{o,y} - B_{21}w_{o,xx} - B_{22}w_{o,yy} + C_{21}\theta_{x,x} + C_{22}\theta_{y,y}$$
$$N_{xy} = A_{66}u_{o,y} + A_{66}v_{o,x} - 2B_{66}w_{o,xy} + C_{66}\theta_{x,y} + C_{66}\theta_{y,x}$$
$$Q_x = C_{11}u_{o,x} + C_{12}v_{o,y} - E_{11}w_{o,xx} - E_{12}w_{o,yy} + G_{11}\theta_{x,x} + G_{12}\theta_{y,y}$$
$$Q_y = C_{21}u_{o,x} + C_{22}v_{o,y} - E_{21}w_{o,xx} - E_{22}w_{o,yy} + G_{21}\theta_{x,x} + G_{22}\theta_{y,y}$$
$$Q_{xy} = C_{66}u_{o,y} + C_{66}v_{o,x} - 2E_{66}w_{o,xy} + G_{66}\theta_{x,y} + G_{66}\theta_{y,x}$$
$$M_x = B_{11}u_{o,x} + B_{12}v_{o,y} - D_{11}w_{o,xx} - D_{12}w_{o,yy} + E_{11}\theta_{x,x} + E_{12}\theta_{y,y}$$
$$M_y = B_{21}u_{o,x} + B_{22}v_{o,y} - D_{21}w_{o,xx} - D_{22}w_{o,yy} + E_{21}\theta_{x,x} + E_{22}\theta_{y,y}$$
$$M_y = B_{21}u_{o,x} + B_{22}v_{o,y} - D_{21}w_{o,xx} - D_{22}w_{o,yy} + E_{21}\theta_{x,x} + E_{22}\theta_{y,y}$$
$$R_x = F_{55}\theta_x$$
$$R_y = F_{44}\theta_y$$

The coefficients of the displacements can be expressed as given in Eq. (18).

$$\{A_{ij}, B_{ij}, C_{ij}, D_{ij}, E_{ij}, G_{ij}\} = \int_{-\frac{h}{2}}^{\frac{h}{2}} \{1, z, f(z), z^2, zf(z), f(z)^2\}\, Q_{ij}\, dz, \tag{14}$$
$$i,j = 1,2,6$$
$$\{F_{ij}\} = \int_{-h/2}^{h/2} \{f'(z)^2\}\, Q_{ij}\, dz$$
$$i,j = 4,5$$

Analytical solution of the partial differential equations given in Eq. (16) can be achieved by the Navier's method based on double Fourier series. According to this method, the displacement field should satisfy the trigonometric functions given in Eq. (19).

$$u_o(x,y,t) = \sum_{m=1}^{\infty}\sum_{n=1}^{\infty} A_{mn}\cos(\alpha x)\sin(\beta y)e^{iwt} \tag{19}$$
$$v_o(x,y,t) = \sum_{m=1}^{\infty}\sum_{n=1}^{\infty} B_{mn}\, sin(\alpha x)\cos(\beta y)\, e^{iwt}$$
$$w_o(x,y,t) = \sum_{m=1}^{\infty}\sum_{n=1}^{\infty} C_{mn}\sin(\alpha x)\sin(\beta y)e^{iwt}$$
$$\theta_x(x,y,t) = \sum_{m=1}^{\infty}\sum_{n=1}^{\infty} T_{xmn}\, cos(\alpha x)\, sin(\beta y)e^{iwt}$$
$$\theta_y(x,y,t) = \sum_{m=1}^{\infty}\sum_{n=1}^{\infty} T_{xmn}\sin(\alpha x)\cos(\beta y)\, e^{iwt}$$

here α and β are $m\pi/a$ and $n\pi/b$, respectively. A_{mn}, B_{mn}, C_{mn}, T_{xmn}, T_{ymn} in Eq. (19) are unknown displacement coefficients. Furthermore, the displacement field should satisfy the following boundary conditions for the simply supported plate.

$$\begin{array}{llll} u_0(x,0,t)=0 & u_o(x,b,t)=0 & v_o(0,y,t)=0 & v_o(a,y,t)=0 \\ w_o(x,0,t)=0 & w_o(x,b,t)=0 & w_o(0,y,t)=0 & w_o(a,y,t)=0 \\ N_y(x,0,t)=0 & N_y(x,b,t)=0 & N_x(0,y,t)=0 & N_x(a,y,t)=0 \\ M_y(x,0,t)=0 & M_y(x,b,t)=0 & M_x(0,y,t)=0 & M_x(a,y,t)=0 \\ \theta_x(x,0,t)=0 & \theta_x(x,b,t)=0 & \theta_y(0,y,t)=0 & \theta_y(a,y,t)=0 \\ Q_y(x,0,t)=0 & Q_y(x,b,t)=0 & Q_x(0,y,t)=0 & Q_x(a,y,t)=0 \\ R_x(x,0,t)=0 & R_x(x,b,t)=0 & R_y(0,y,t)=0 & R_y(a,y,t)=0 \end{array} \tag{2}$$

The distributed dynamic load in the direction of gravity can be defined as

$$q(x,y,t) = \sum_{m=1}^{\infty}\sum_{n=1}^{\infty} Q_{mn}(t)\ sin\left(\frac{m\pi x}{a}\right) sin\left(\frac{n\pi y}{b}\right) \tag{31}$$

$$Q_{mn}(t) = \frac{4}{ab}\int_{-a/2}^{a/2}\int_{-b/2}^{b/2} q(x,y,t)\, sin\left(\frac{m\pi x}{a}\right) sin\left(\frac{n\pi y}{b}\right) dydx \tag{4}$$

Time-dependent functions can be transformed into linear algebraic functions by means of Laplace transform. This transformation simplifies the solution as it eliminates the requirement of determining a suitable time step. The details of the Laplace transform can be found in many studies available in the literature (Calim 2003, Reddy 2013, Eratlı *et al.* 2014, Calim 2016, Cuma and Calim 2021a, Calim and Cuma 2022, 2023, Turker *et al.* 2023, Özbey *et al.* 2024). If the Laplace transforms of the equations of motion are given in matrix form the following system of matrices can be obtained.

$$\left(\begin{bmatrix} k_{11} & k_{12} & k_{13} & k_{14} & k_{15} \\ . & k_{22} & k_{23} & k_{24} & k_{25} \\ . & . & k_{33} & k_{34} & k_{35} \\ . & . & . & k_{44} & k_{45} \\ . & . & . & . & k_{55} \end{bmatrix} + s^2\begin{bmatrix} m_{11} & m_{12} & m_{13} & m_{14} & m_{15} \\ . & m_{22} & m_{23} & m_{24} & m_{25} \\ . & . & m_{33} & m_{34} & m_{35} \\ . & . & . & m_{44} & m_{45} \\ . & . & . & . & m_{55} \end{bmatrix}\right)\begin{bmatrix} \bar{A}_{mn} \\ \bar{B}_{mn} \\ \bar{C}_{mn} \\ \bar{T}_{xmn} \\ \bar{T}_{ymn} \end{bmatrix} = \begin{bmatrix} \bar{P}_x \\ \bar{P}_y \\ \bar{Q}_{mn} \\ \bar{m}_x \\ \bar{m}_y \end{bmatrix} \tag{5}$$

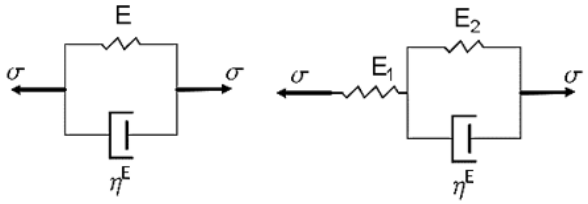

(a) (b)

Fig. 3 (a) Kelvin model and (b) Linear standard model

here s is the Laplace transform parameter. In closed form Eq. (23) can be shown as follows

$$[\boldsymbol{K_{mn}} + s^2\, \boldsymbol{M_{mn}}]\, \bar{\boldsymbol{D}}_{\boldsymbol{mn}} = \bar{\boldsymbol{F}}_{\boldsymbol{mn}} \tag{6}$$

where $\bar{\mathbf{D}}_{\boldsymbol{mn}}$ is the unknown displacement vector and $\bar{\mathbf{F}}_{\boldsymbol{mn}}$ is the external force vector in Laplace domain.

The unknown displacements determined by the solution of Eq. (24) are in Laplace domain which must be transformed into time domain. Therefore, Durbin's modified inverse Laplace transform procedure is employed. Durbin's equation for the inverse Laplace transform

$$f(t_j) \cong \frac{2\, e^{ajt}}{T}\left[-\frac{1}{2} Re\{\bar{F}(a)\} + Re\left\{\sum_{k=0}^{N-1}\{\bar{F}(s_k)\, L_k\, e^{i\left(\frac{2\pi}{N}\right)j\,k}\right\}\right] \tag{7}$$

$$L_k = 1\ for\ k = 0\ ;$$
$$L_k = \frac{sin\left(\frac{k\pi}{N}\right)}{\frac{k\pi}{N}}\ for\ k > 0 \tag{26}$$

here "L_k" is Lanczos factor, "i" is complex number, "s_k" is the k^{th} Laplace transform parameter which is $a + i\frac{2\pi k}{T}$, where T is the total solution time and N is the number of time segments. $t_j = j\Delta t = jT/N, (j = 0, 1, 2, \ldots, N-1)$ is used for the calculation of $f(t_j)$. Value of "aT" is known to be between 5 and 10. Furthermore, it is observed from previous studies (Calim 2003, Temel *et al.* 2004, Temel and Şahan 2018, Cuma and Calim 2021b) optimum value for "aT" is determined as 6.

Forced vibration analysis can be carried out with or without the damping effect. Although the elastic vibration case is simpler to implement, viscoelastic material models yield more realistic results. Therefore, various viscoelastic models are presented in the literature. In this study, two of the most popular viscoelastic models are used: Kelvin viscoelastic model and linear standard viscoelastic model. Each viscoelastic model presents its own viscoelastic material properties that can be integrated into the solution by the correspondence principle. Boley and Weiner (1960) demonstrated the correspondence principle which states that the viscoelastic constants can be used instead of elastic constants.

Kelvin viscoelastic model can be seen in Fig. 3. (a). By using the elastic-viscoelastic analogy, the elastic constants in Kelvin model can be replaced by (Calim 2003, Temel *et al.* 2004, Eratli *et al.* 2014, Cuma and Claim 2022)

$$E_v(z) = E(z)(1 + g\, s), \tag{8}$$

$$G_v(z) = G(z)(1 + g\, s)$$

where E_v and G_v are viscoelastic elasticity and shear modulus, respectively. g is damping ratio and s is the Laplace parameter. By using the correspondence principle viscoelastic material properties are directly used in the algorithm.

Linear standard model can be seen Fig. 2(b) viscoelastic material parameters for this model can be expressed as (Eratli *et al.* 2014)

$$\bar{E}_v(z) = E(z)\left(\frac{1 + \beta^G \tau_r^G s}{1 + \tau_r^G s}\right),$$
$$\bar{G}_v(z) = G(z)\left(\frac{1 + \beta^G \tau_r^G s}{1 + \tau_r^G s}\right) \tag{9}$$

β^G and τ_r^G are the ratio of instantaneous value and retardation time of the relaxation function for the linear standard model. Also, $\bar{E}_v(\mathrm{z})$ and $\bar{G}_v(\mathrm{z})$ represent the viscoelastic shear modulus and the modulus of elasticity, respectively. The ratio of instantaneous value and retardation time of the relaxation function are given as follows.

$$\tau_r^G = \frac{\eta^E}{E_1 + E_2} \qquad \beta^G = \frac{E_1 + E_2}{E_2} > 1 \tag{10}$$

3. Numeric examples

In this study, dynamic behaviour of FGM and PFG plates resting on elastic foundation is examined and obtained results are compared with examples available in the literature. The properties used in the examples are given in Table 1.

Free vibration analysis of FGM and PFG plates resting on elastic foundation is carried out and results are compared with Akavci (2014), Shahsavari *et al.* (2018) and Van *et al.* (2021). Subsequently, verification of forced vibration of viscoelastic FGM plates is done by comparison with Dogan (2022). Finally, a parametric study is conducted for the damped forced vibration of VPFG plates resting on elastic foundation. Obtained results are given in graphical form.

Some values of porosity volume index may result in negative elasticity modulus. Perceiving the limits of ξ in order to prevent negative material properties is required. Therefore, a study was conducted to determine the effect of porosity and power-law exponent on the modulus of elasticity. The obtained results are given in Fig 4.

Fig. 4 shows the change in Young's modulus by the porosity volume index. Fig. 4(a) considers $p = 0$ and *PD-I* case, where material gradient is 0 and Young's modulus is constant throughout the thickness for all ξ. Fig. 4(b) involves a linear change in Young's modulus due to the power law index $p = 1$. Furthermore, the effect of porosity volume index is also present in this case. As can be seen, lowest values of Young's modulus are encountered in this case. Fig. 4(c) and 4(d) suggest that the effect of porosity volume index in *PD-II* cases have limited impact on Young's modulus. Finally, Fig. 4(b) indicates that if the porosity volume index gets higher than 0.3, Young's modulus decreases to negative values. In order to avoid

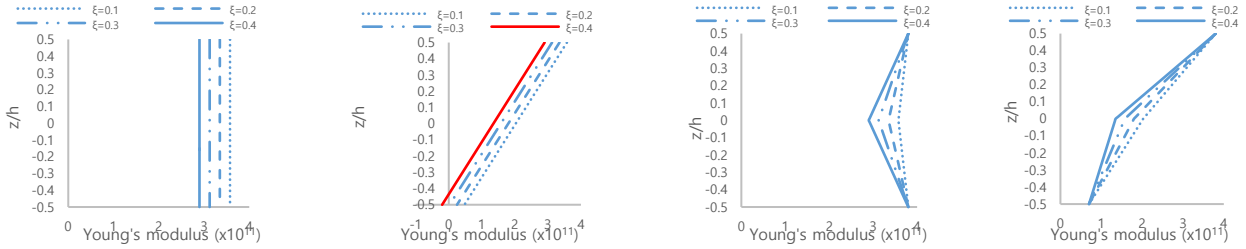

(a) *PD-I*, p=0 (b) *PD-I* and p=1 (c) *PD-II* and p=0 (d) *PD-II* and p=1

Fig. 4 Change in Young's moduli via the thickness

Table 2 Frequency parameters $\bar{\omega}$ for PFG rectangular plates

K_0, K_1	a/h	Perfect			PD-I					PD-II				
		$\xi = 0$			$\xi = 0.1$	$\xi = 0.2$			$\xi = 0.3$	$\xi = 0.1$	$\xi = 0.2$			$\xi = 0.3$
		Akavci (2014)	Shahsavari *et al.* (2018)	Present Study	Present Study	Van *et al.* (2021)	Shahsavari *et al.* (2018)	Present Study	Present Study	Present Study	Van *et al.* (2021)	Shahsavari *et al.* (2018)	Present Study	Present Study
(0,0)	5	8.037	8.151	8.037	7.826	7.497	7.641	7.553	7.161	8.048	7.904	8.164	8.057	8.064
	10	8.690	8.818	8.690	8.431	8.015	8.203	8.103	7.646	8.709	8.497	8.845	8.729	8.748
	20	8.888	9.020	8.888	8.613	8.163	8.370	8.267	7.789	8.910	8.667	9.052	8.934	8.957
(100,0)	5	8.475	8.577	8.475	8.323	8.057	8.203	8.126	7.844	8.507	8.378	8.636	8.540	8.573
	10	9.111	9.231	9.111	8.911	8.574	8.753	8.661	8.315	9.150	8.969	9.301	9.19	9.237
	20	9.304	9.430	9.304	9.089	8.723	8.917	8.821	8.455	9.347	9.139	9.505	9.393	9.442
(100,100)	5	14.641	14.640	14.641	15.074	16.369	15.595	15.591	16.213	15.188	14.904	15.192	15.188	15.496
	10	15.193	15.245	15.193	15.607	16.015	16.148	16.112	16.731	15.766	15.586	15.812	15.766	16.090
	20	15.367	15.439	15.367	15.773	16.21	16.32	16.271	16.885	15.646	15.794	16.011	15.949	16.280

Table 1 Material features used in study

Material	Properties		
	$\rho\ (kg/m^3)$	$E(GPa)$	ν
Alumina (Al_2O_3)	3800	380	0.3
Aluminium (Al)	2702	70	0.3

negative values of Young's modulus maximum porosity volume index is chosen as 0.3 for all of analysis.

3.1 Free vibration analysis of PFG plate

Free vibration analysis of rectangular PFG plates resting on elastic foundation is carried out. Perfect and porous plates are taken into consideration. Material properties given in Table 1 are used. Calculation of the fundamental frequencies is done for $a = b = 1\ m$ and $p = 1$. The effect of various thickness ratios $(a/h = \{5, 10, 20\})$, porosity volume indexes $(\xi = 0, 0.1, 0.2, 0.3)$ and stiffness parameters of foundation $(K_0, K_1 = \{0, 0\}, \{100, 0\}, \{100, 100\})$ are investigated. Obtained results are compared with the ones available in the literature and given in tabular form.

Non-dimensional fundamental frequencies and non-dimensional parameter of foundation are

$$\breve{\omega} = \omega\ \frac{a^2}{h}\sqrt{\frac{\rho_m}{E_m}}, k_0 = \frac{K_0\ D_0}{a^4}, k_1 = \frac{K_1\ D_0}{a^2}, D_0 = \frac{E_m\ h^3}{12\ (1-\upsilon_m{}^2)} \tag{11}$$

The non-dimensional fundamental frequencies given in Table 2 show that the results obtained from present study are compatible with ones available in the literature.

3.2 Forced vibration analysis of FGM plate

In this example, damped forced vibration of simply supported FGM rectangular plates is analysed. Dogan (2022) used FSDT for the solution of this problem while HSDT is used in the present study. A uniformly distributed impulsive step load is applied on the FGM plate. Calculation of load vector and dynamic stiffness matrices are performed in Laplace domain. Subsequently, results are converted to time domain by using Durbin's modified inverse Laplace transform algorithm. The following parameters are used in this example; $a = b = 0.2\ m$, $h = 0.01\ m$, $g = (0, 1\ e^{-5}, 3\ e^{-5},\ 5\ e^{-5})$, $p = (1, 2, 5)$ and $q_0 = 10^6\ \mathrm{N}/m^2$. Material properties used in this analysis are given in Table 1. Obtained results are given in comparison in Fig. 5. Non-dimensional time (t') and non-dimensional displacement (w') parameters can be expressed as (Reddy 2000, Hajlaoui *et al.* 2017)

$$t' = t\sqrt{\frac{E_m}{a^2\rho_m}} \qquad w' = \frac{E_m h}{a^2 q_0} \tag{31}$$

As can be seen from Fig. 5, as power-law exponent increases, non-dimensional center deflection increases. This can be attributed to the fact wiih an increase in power-law exponent, the material transitions more rapidly from

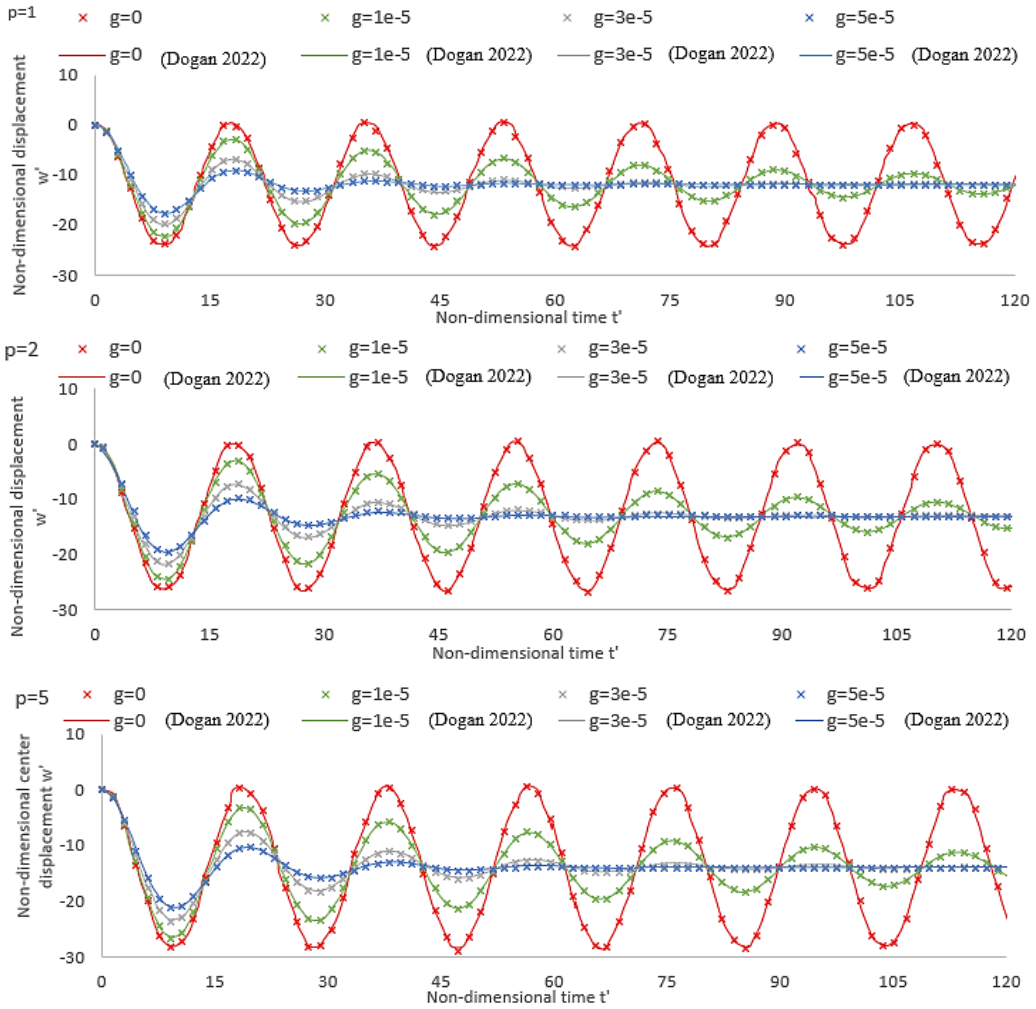

Fig. 5 Effect of various power-law exponent (p) and damping ratio (g) to center displacement by comparing present study and Dogan (2022)

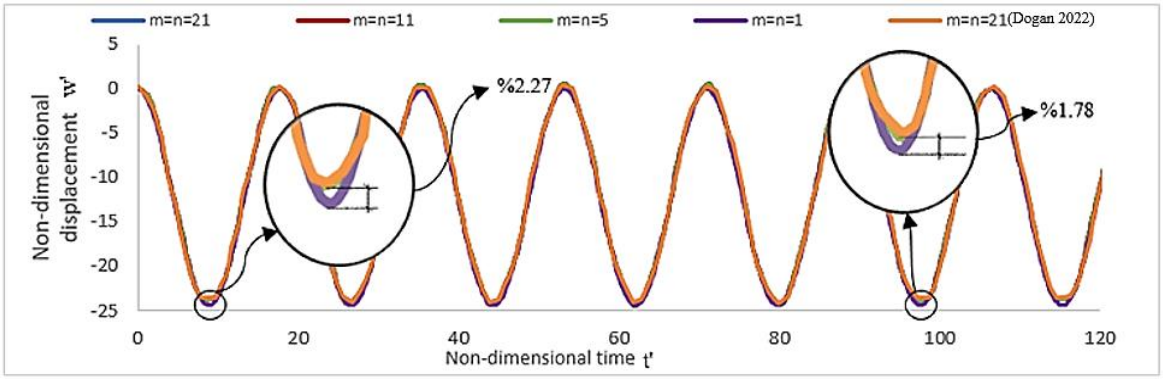

Fig. 6 Effect of various Fourier coefficients (m and n) to center displacement for $g = 0$

ceramic, which has a higher Young's modulus, to metal, which has a lower Young's modulus. In addition, non-dimensional center deflection decreases while the damping ratio increases. In Fig. 5, the concordance between the results of the present study and Dogan (2022) is evident. In addition, a study is conducted in order to determine the required number of terms for the Fourier series. Result of this study is given in Fig. 6.

Fig. 6 shows the difference between the minimum (1) and maximum (21) number of terms taken in Fourier series in percentage. Although the results of 21 terms and 1 term of the Fourier series are noticeably differ, required accuracy can be achieved by taking 11 terms or even 5 terms from Fourier series. The computational encumbrance can be reduced by taking 5 terms for the Fourier series.

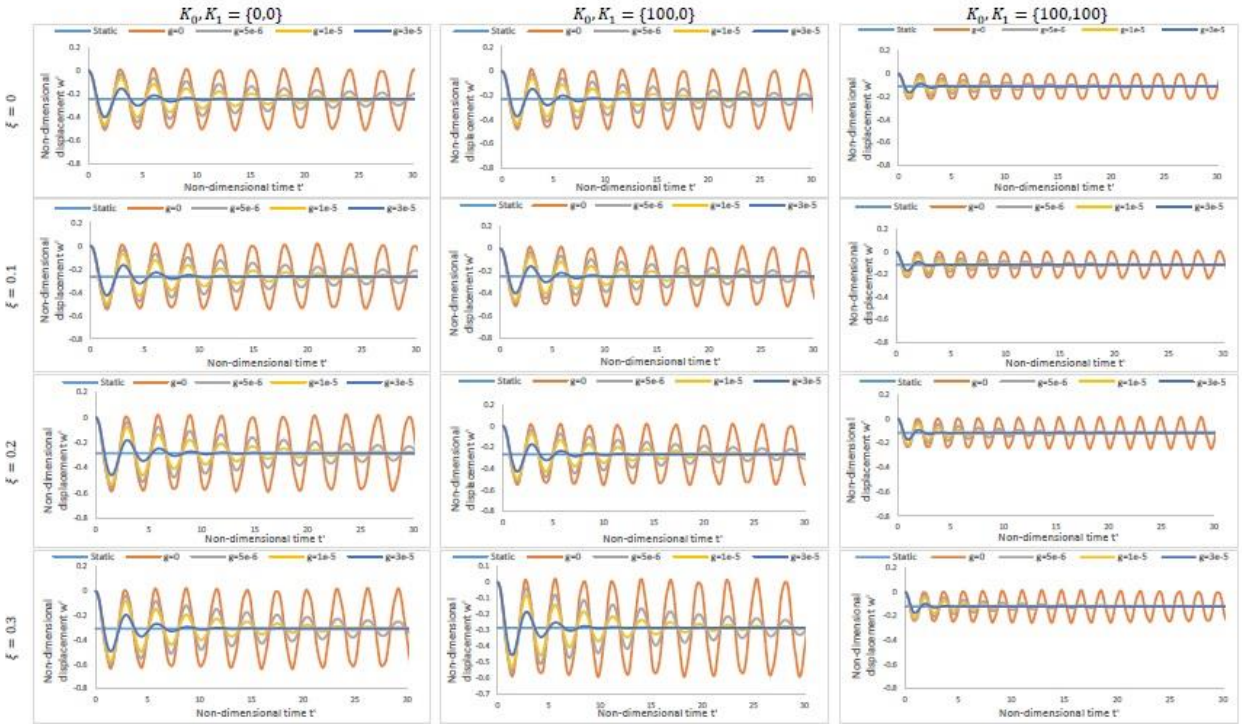

Fig. 7 Non-dimensional displacement at the center point of rectangular plate ($p = 0$, *PD-I*)

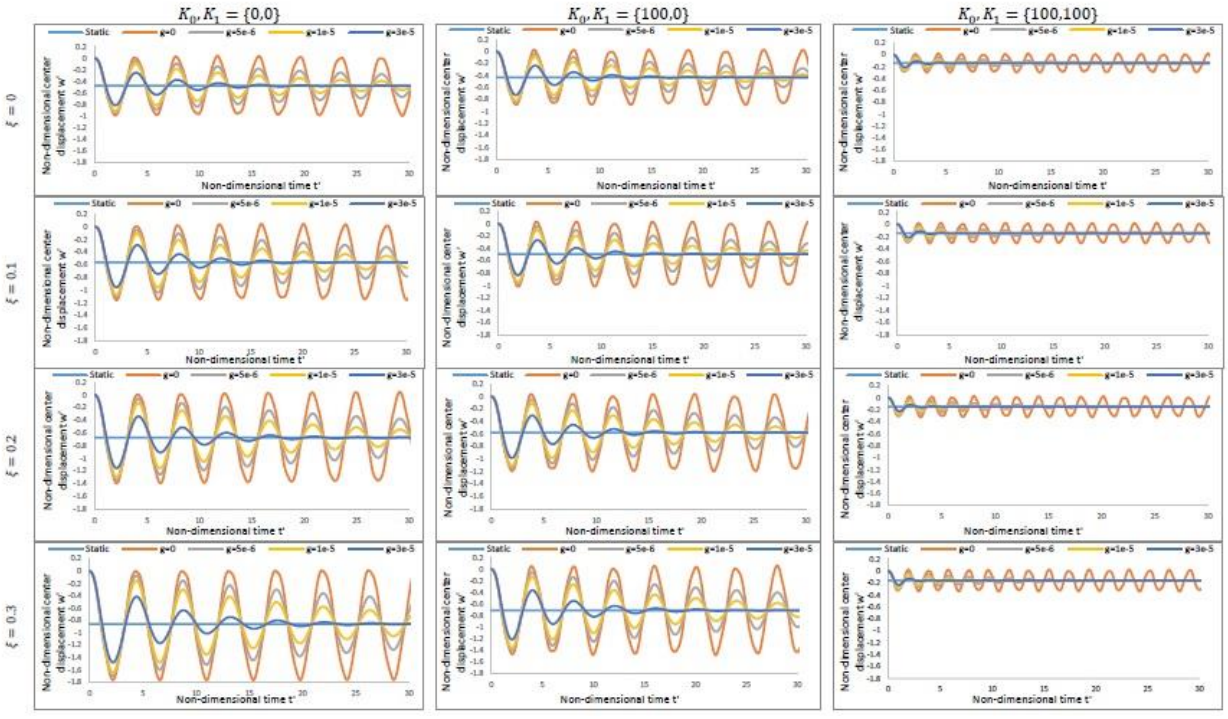

Fig. 8 Non-dimensional displacement at the center point of rectangular plate ($p = 1$, *PD-I*)

3.3 Forced vibration analysis of VPFG plate

3.3.1 Kelvin model

In this parametric study, damped forced vibration behaviour of VPFG plates resting on elastic foundation is investigated. Free vibration analysis of this problem was solved by Shahsavari *et al.* (2018). Material properties used are given in Table 1. Constant geometrical properties are $a = b = 1\ m$, $h/a = 0.2$.

Two porosity functions given in Eqs. (1) and (2) are implemented and effects of various porosity volume indexes ($\xi = 0, 0.1, 0.2, 0.3$) , stiffness parameters of foundation $(K_0, K_1 = 0{,}0{,}100{,}0{,}100{,}100)$, damping ratios

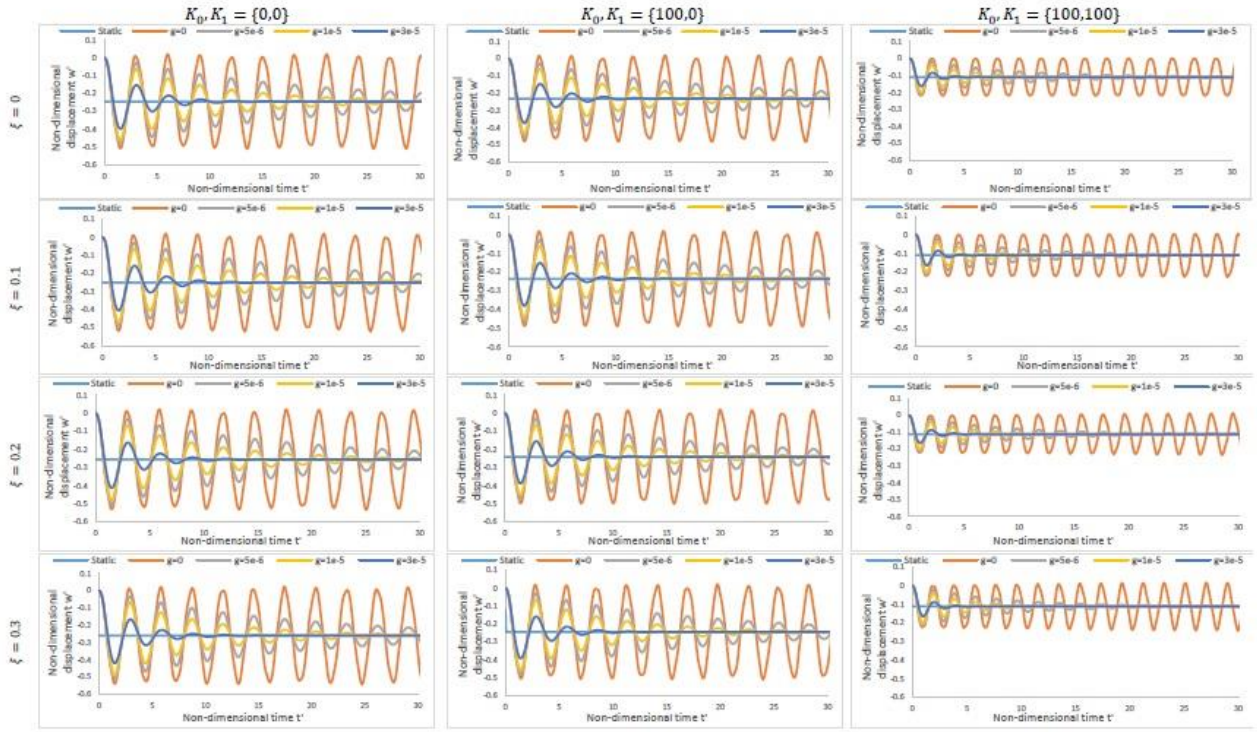

Fig. 9 Non-dimensional displacement at the center point of rectangular plate ($p = 0$, *PD-II*)

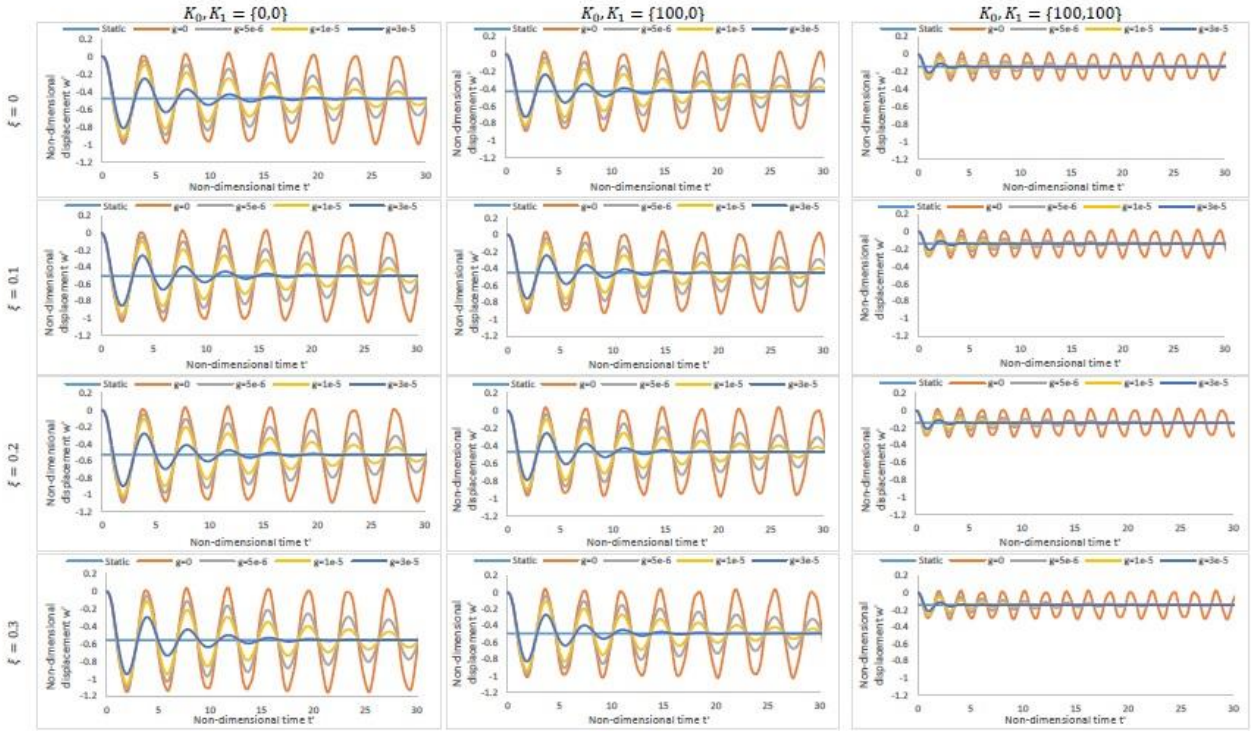

Fig. 10 Non-dimensional displacement at the center point of rectangular plate ($p = 1$, *PD-II*)

($g = 5\,e^{-6}, 1\,e^{-5},\ 3\,e^{-5}$) and power-law exponents ($p = 0,1$) are examined. Obtained results are presented in graphical form. Same distributed load and non-dimensional transformation functions used in example 2 is also employed for this parametric study.

By inspecting the Figs. 7-10, following results can be obtained. As the stiffness parameters of foundation increase, displacement decreases as expected. The effect of Pasternak layer is clearly higher than Winkler layer. As damping ratio increases, the dominance of the viscoelastic behaviour has

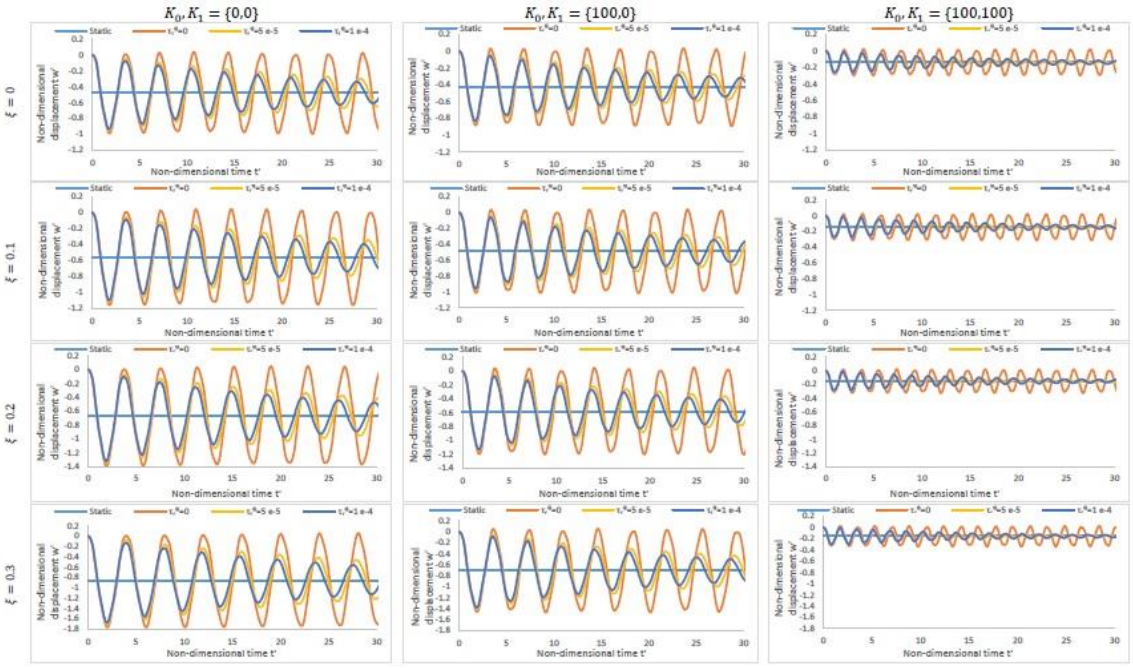

Fig. 11 Non-dimensional displacement at the center point of rectangular plate ($\beta^G = 1.1$, *PD-I*)

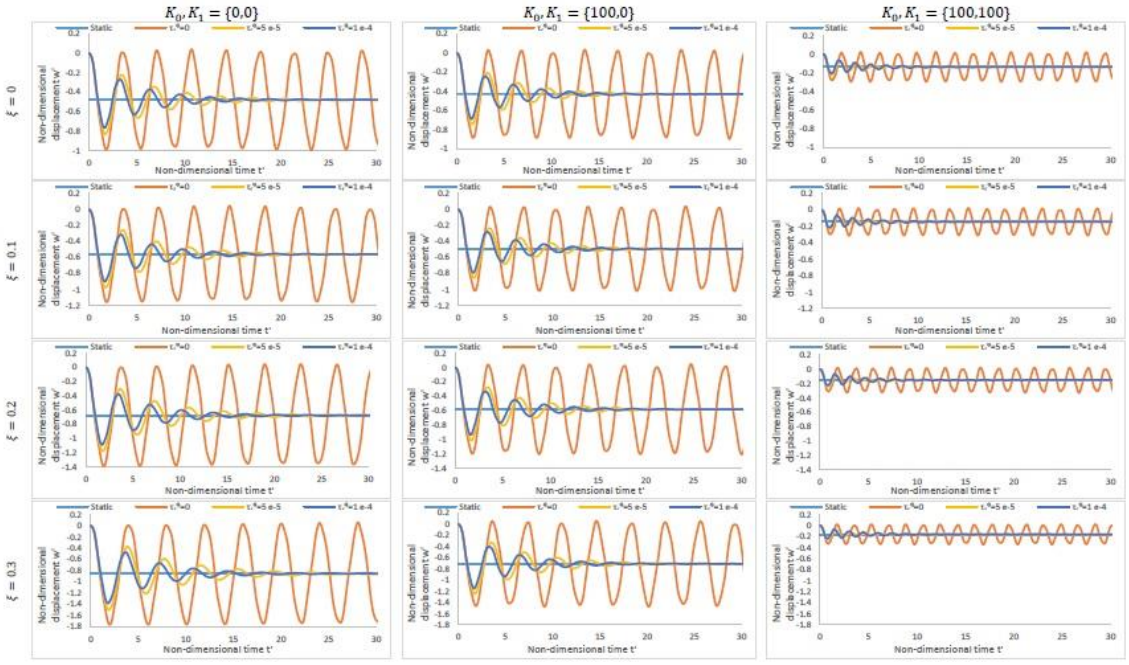

Fig. 12 Non-dimensional displacement at the center point of rectangular plate ($\beta^G = 1.5$, *PD-I*)

higher effect on the motion. Therefore, the dissipation of the displacements increases as expected. Power-law exponent controls the material changes between metal and ceramic. In this example increase in p, results faster transition to metal. Therefore, displacements increase.

Fig. 7 indicates that the change in displacement amplitudes due to porosity volume index is meagre without the effect of power law index. Subsequently, as can be seen from Fig. 8, effect of the porosity volume index increases when combined with the effect of power law index. Although, the porosity volume indexes are identical in all cases. Figs. 9 and 10 suggest that their effect is limited in *PD-II* case due to small change in Young's modulus which can be seen in Fig. 4.

Period decreases due to the increase in stiffness parameters of foundation. Porosity volume index decreases the period in all cases other than $n = 1$ and *PD-I* case. As can be seen in Fig. 8, the periods increase as a result of Young's modulus reaching the lowest values.

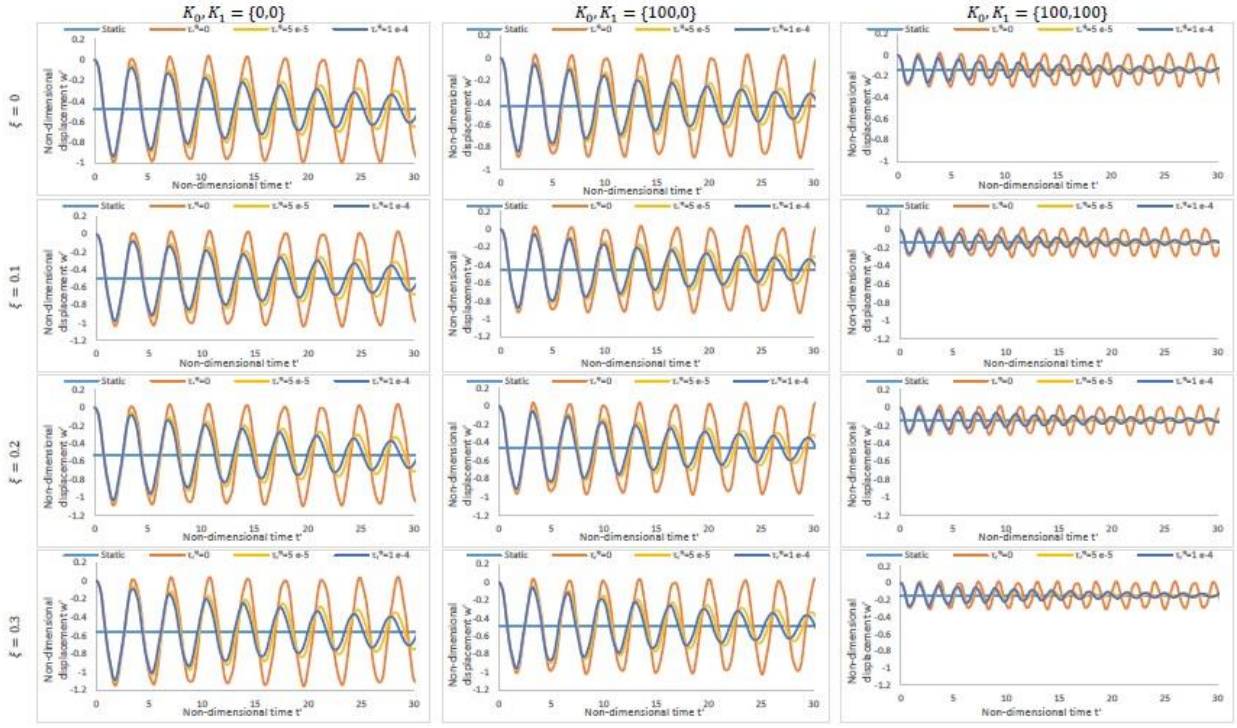

Fig. 13 Non-dimensional displacement at the center point of rectangular plate ($\beta^G = 1.1$, *PD-II*)

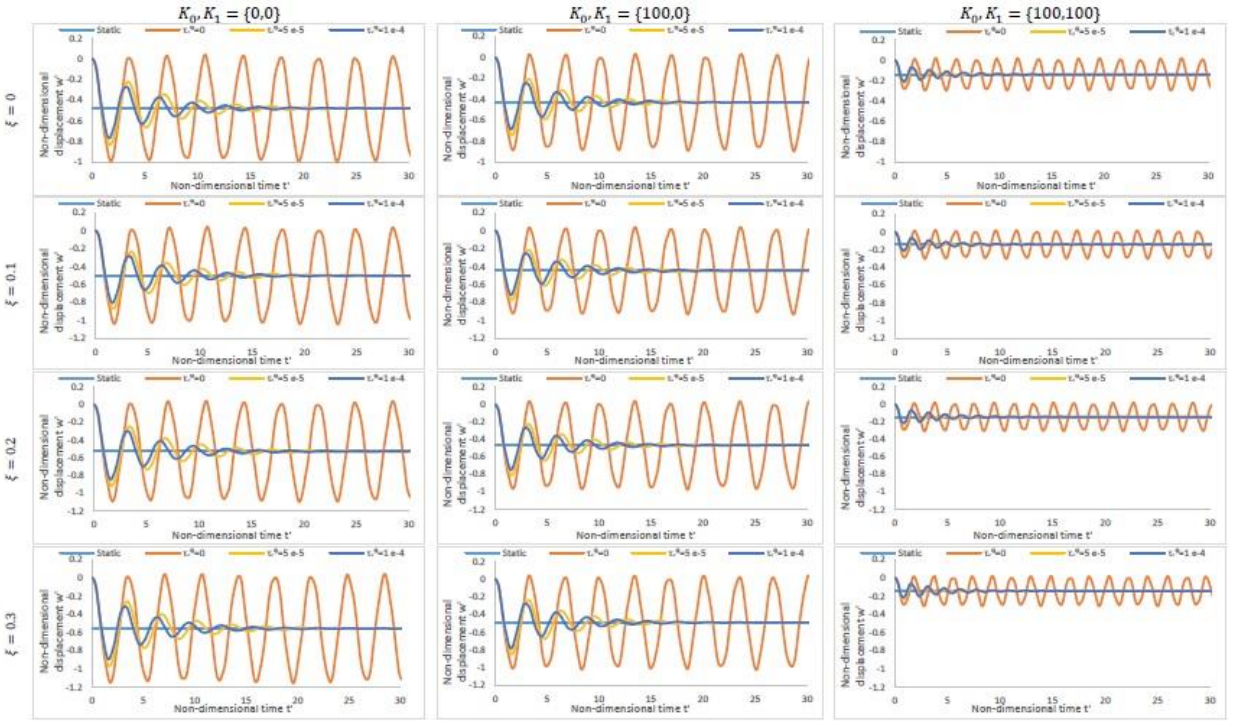

Fig. 14 Non-dimensional displacement at the center point of rectangular plate ($\beta^G = 1.5$, *PD-II*)

3.3.2 Linear standard model

In this parametric study, the effect of linear standard model on VPFG plates resting on elastic foundation is investigated. Material properties used are given in Table 1. Constant geometrical properties are $a = b = 1\,m$, $h/a = 0.2$.

Two porosity functions given in Eqs. (1) and (2) are implemented and effects of various porosity volume fraction indexes ($\xi = 0, 0.1, 0.2, 0.3$), stiffness parameters of foundation ($K_0, K_1 = \{0,0\}, \{100,0\}, \{100,100\}$), the ratio of instantaneous value($\beta^G = 1.1$,1.5) and retardation time of the relaxation function ($\tau_r^G = 0, 5\,e^{-5}, 1\,e^{-4}$) are

examined. Analyses are performed for $p = 1$ .Obtained results are presented in graphical form.

Distributed load and non-dimensional transformation functions used in example 2 is also employed for this parametric study. Obtained results are given in graphical form in Figs. 11-14.

By inspecting the Figs. 11-14, following results can be obtained. The change in displacements is conspicuous as the power law index in all cases of this example is 1. As expected, the displacements decrease contrary to the stiffness parameters of foundation. The effect of Pasternak layer is clearly higher than Winkler layer. Due to the decrease of the effective modulus of elasticity via the increase of porosity volume index, the displacements also increase in this parametric example. Furthermore, the increase of the displacements in *PD-I* case are more prominent in comparison to *PD-II* case.

As the parameters of linear standard model increase, the displacement decreases. Additionally, increase of the instantaneous value of relaxation function β^G dissipates the oscillations faster than the increase of the retardation time of relaxation function τ_r^G . Period decreases due to the increase in stiffness parameters of foundation. However, Pasternak layer affects the periods further than the Winkler layer. Although, τ_r^G and β^G both reduce the periods, the effect of β^G is more apparent. Furthermore, porosity volume index increases the periods in *PD-I* case, however, its effect is negligible in *PD-II* case.

4. Conclusions

In this paper, dynamic behaviour of simply supported viscoelastic porous functionally graded rectangular plate resting on elastic foundation is investigated. The equations of motion are derived by the energy method and Hamilton's principle. Navier's method based on double Fourier series is employed for the solution. Free vibration of PFG plates and forced vibration of FGM plates are analysed and the results are compared with the studies available in the literature. Subsequently, two parametric studies for the damped forced vibration of PFG plates resting on elastic foundation considering Kelvin and linear standard viscoelastic models are carried out. The results are given in graphical form. The conclusions from the analysis are as follows.

• The increase in stiffness parameters of foundation causes a decrease in displacements as a result of increasing stiffness. The effect of Pasternak layer (K_1) is clearly higher than Winkler layer (K_0).

• Since the increase in porosity volume index causes a decrease in effective modulus of elasticity, displacements increase. However, the effect of ξ is limited without the effect of power law index.

• For the examples in this study, power law exponent quickens the transition from ceramic to metal. Thus, displacements increase while Young's modulus decreases.

• While the Young's modulus reaches lower values, period increases. On the contrary, as Young's modulus transitions from metal to ceramic, the period decrease.

• FGM and porosity volume indexes parameters affect displacements at the rate of changing the material parameter. The more effective the material change, the greater displacement change.

• For the Kelvin model, the increase in the damping ratio accelerates the decrease in displacements as the dominance of viscoelastic behaviour on the motion increases.

• For *PD-I* and *PD-II* of Kelvin model, the change in displacement amplitudes due to porosity volume index is meagre without the effect of power law index. Subsequently, effect of the porosity volume index increases when combined with the effect of power law index.

• For *PD-II*, although, the porosity volume indexes are identical in all cases, their effect is limited due to small change in Young's modulus.

For the linear standard model, the effect of β^G on the amplitudes and the dissipation of displacements are significantly higher than τ_r^G. As the parameters of the linear standard model increase, displacement and period decrease.

References

Akavci, S.S. (2014), "An efficient shear deformation theory for free vibration of functionally graded thick rectangular plates on elastic foundation", *Compos. Struct.*, **108**, 667-676. https://doi.org/10.1016/j.compstruct.2013.10.019.

Akavci, S.S. and Tanrikulu, A.H. (2015), "Static and free vibration analysis of functionally graded plates based on a new quasi-3D and 2D shear deformation theories", *Compos. B Eng.*, **83**, 203-215. https://doi.org/10.1016/j.compositesb.2015.08.043.

Alavi, S.K., Ayatollahi, M.R., Petrů, M. and Koloor, S.S.R. (2022), "On the dynamic response of viscoelastic functionally graded porous plates under various hybrid loadings", *Ocean Eng.*, **264**, 112541. https://doi.org/10.1016/j.oceaneng.2022.112541.

Alnujaie, A., Akbas, S.D., Eltaher, M.A. and Assie, A. (2021), "Forced vibration of a functionally graded porous beam resting on viscoelastic foundation", *Geomech. Eng.*, **24**(1), 91-103. https://doi.org/10.12989/gae.2021.24.1.091.

Arefi, M. and Meskini, M. (2019), "Application of hyperbolic shear deformation theory to free vibration analysis of functionally graded porous plate with piezoelectric face-sheets", *Struct. Eng. Mech.*, **71**(5), 459-467 https://doi.org/10.12989/sem.2019.71.5.459.

Baferani, A.H., Saidi, A.R. and Ehteshami, H. (2011), "Accurate solution for free vibration analysis of functionally graded thick rectangular plates resting on elastic foundation", *Compos. Struct.*, **93**, 1842-1853. https://doi.org/10.1016/j.compstruct.2011.01.020.

Bardell, N.S. (1991), "Free vibration analysis of a flat plate using the hierarchical finite element method", *J. Sound Vib.*, **151**, 263-289. https://doi.org/10.1016/0022-460X(91)90855-E.

Benahmed, A., Houari, M.S.A., Benyoucef, S., Belakhdar, K. and Tounsi, A. (2017), "A novel quasi-3D hyperbolic shear deformation theory for functionally graded thick rectangular plates on elastic foundation", *Geomech. Eng.*, **12(1),** 9-34. https://doi.org/10.12989/gae.2017.12.1.009.

Boley, B.A., Weiner J.H. (1960), "Theory of thermal stresses", New York: *John Wiley & Sons, Ltd.*

Boulefrakh, L., Hebali, H., Chikh, A., Bousahla, A.A., Tounsi, A. and Mahmoud, S.R. (2019), "The effect of parameters of visco-Pasternak foundation on the bending and vibration properties of a thick FG plate", *Geomech. Eng.*, **18**(2), 161-178. https://doi.org/10.12989/gae.2019.18.2.161.

Burlayenko, V.N., Altenbach, H. and Sadowski, T. (2015), "An evaluation of displacement-based finite element models used for

free vibration analysis of homogeneous and composite plates", *J. Sound Vib.*, **358**, 152-175 https://doi.org/10.1016/j.jsv.2015.08.010.

Calim, F.F. (2003), "Dynamic analysis of viscoelastic, anisotropic curved spatial rod systems", Ph. D. Dissertation, *Cukurova University*, Adana, Turkey, **160**.

Calim, F.F. (2016), "Dynamic response of curved Timoshenko beams resting on viscoelastic foundation." *Struct. Eng. Mech.*, **59**(4), 761–774. http://dx.doi.org/10.12989/sem.2016.59.4.761

Calim, F.F. and Cuma, Y.C. (2022), "Vibration analysis of nonuniform hyperboloidal and barrel helices made of functionally graded material", *Mech. Based Des. Struct.*, **50**(11), 3781-3795 https://doi.org/10.1080/15397734.2020.1822181.

Calim, F.F. and Cuma, Y.C. (2023), "Forced vibration analysis of viscoelastic helical rods with varying cross-section and functionally graded material", *Mech. Based Des. Struct.*, **51**(7), 3620-3631 https://doi.org/10.1080/15397734.2021.1931307.

Chikr, S.C., Kaci, A., Bousahla, A.A., Bourada, F., Tounsi, A., Bedia, E.A., Mahmoud, S.R., Benrahou, K.H. and Tounsi, A. (2020), "A novel four-unknown integral model for buckling response of FG sandwich plates resting on elastic foundations under various boundary conditions using Galerkin's approach", *Geomech. Eng.*, **21**(5), 471-487. https://doi.org/10.12989/gae.2020.21.5.471.

Cho, K.N., Bert, C.W. and Striz, A.G. (1991), "Free vibrations of laminated rectangular plates analyzed by higher order individual-layer theory", *J. Sound Vib.*, **145**, 429-442 https://doi.org/10.1016/0022-460X(91)90112-W.

Choe, K., Tang, J., Shui, C., Wang, A. and Wang, Q. (2018), "Free vibration analysis of coupled functionally graded (FG) doubly-curved revolution shell structures with general boundary conditions", *Compos. Struct.*, **194**, 413-432 https://doi.org/10.1016/j.compstruct.2018.04.035.

Cuma, Y.C. and Calim, F.F. (2021a). Free vibration analysis of functionally graded cylindrical helices with variable cross-section." *J. Sound Vib.*, **494**, 115856. https://doi.org/10.1016/j.jsv.2020.115856

Cuma, Y.C. and Calim, F.F. (2021b), "Transient response of functionally graded non-uniform cylindrical helical rods", *Steel Compos. Struct.*, **40**(4), 571-580 https://doi.org/10.12989/scs.2021.40.4.571.

Cuma, Y.C. and Calim, F.F. (2022), "Dynamic response of viscoelastic functionally graded barrel and hyperboloidal coil springs with variable cross-sectional area", *Mech. Time Depend. Mater*., **26**, 923-937. https://doi.org/10.1007/s11043-021-09520-1.

Cuma, Y.C., Özbey, M.B. and Calim, F.F. (2023), "Vibration and damping analysis of functionally graded shells", *Mech. Time Depend. Mater*., https://doi.org/10.1007/s11043-023-09621-z.

Dogan, A. (2022), "Quasi-static and dynamic response of functionally graded viscoelastic plates", *Compos. Struct.*, **280**, 114883. https://doi.org/10.1016/j.compstruct.2021.114883.

Eratlı, N., Argeso, H., Calim, F.F., Temel, B., Omurtag, M.H. (2014), "Dynamic analysis of linear viscoelastic cylindrical and conical helicoidal rods using the mixed FEM", *J. Sound Vib*., **333**, 3671-3690. https://doi.org/10.1016/j.jsv.2014.03.017.

Hajlaoui, A., Triki, E., Frikha, A., Wali, M. and Dammak, F. (2017), "Nonlinear dynamics analysis of FGM shell structures with a higher order shear strain enhanced solid-shell element", *LAJSS*, **14**, 72–91 https://doi.org/10.1590/1679-78253323.

Kumar, S., Ranjan, V. and Jana, P. (2018), "Free vibration analysis of thin functionally graded rectangular plates using the dynamic stiffness method", *Compos. Struct*., **197**, 39-53. https://doi.org/10.1016/j.compstruct.2018.04.085.

Leissa, A.W. (1973), "The free vibration of rectangular plates", *J. Sound Vib*., **31**, 257-293. https://doi.org/10.1016/S0022-460X(73)80371-2.

Mantari, J.L., Granados, E.V., Hinostroza, M.A. and Soares, C.G. (2014), "Modelling advanced composite plates resting on elastic foundation by using a quasi-3D hybrid type HSDT", *Compos. Struct*., **118**, 455-471. https://doi.org/10.1016/j.compstruct.2014.07.039.

Matsunaga, H. (2008), "Free vibration and stability of functionally graded plates according to a 2-D higher-order deformation theory", *Compos. Struct*., **82**, 499-512. https://doi.org/10.1016/j.compstruct.2007.01.030.

Messina, A. (2011), "Influence of the edge-boundary conditions on three-dimensional free vibrations of isotropic and cross-ply multilayered rectangular plates", *Compos. Struct*., **93**, 2135-2151. https://doi.org/10.1016/j.compstruct.2010.11.010.

Nagino, H., Mikami, T. and Mizusawa, T. (2008), "Three-dimensional free vibration analysis of isotropic rectangular plates using the B-spline Ritz method", J. *Sound Vib.*, **317**, 329-353. https://doi.org/10.1016/j.jsv.2008.03.021.

Nebab, M., Benguediab, S., Atmane, H.A. and Bernard, F. (2020), "A simple quasi-3D HDST for dynamic behavior of advanced composite plates with the effect of variables elastic foundations", *Geomech. Eng*., **22**(5), 415-431. https://doi.org/10.12989/gae.2020.22.5.415.

Nedri, K., Meiche, N.E. and Tounsi, A. (2014), "Free vibration analysis of laminated composite plates resting on elastic foundations by using a refined hyperbolic shear deformation theory", *Mech. Compos. Mater*., **49**, 629-640, https://doi.org/10.1007/s11029-013-9379-6.

Neves, A.M.A., Ferreira, A.J.M., Carrera, E., Roque, C.M.C., Cinefra, M. and Jorge, R.M.N. (2012), "A quasi-3D sinusoidal shear deformation theory for the static and free vibration analysis of functionally graded plates", *Compos. B Eng*., **43**, 711-725. https://doi.org/10.1016/j.compositesb.2011.08.009.

Özbey, M. B., Cuma, Y. C., Deneme, I.O. and Calim, F. F. (2024), "Free and forced vibration analysis of FG-CNTRC viscoelastic plate using high shear deformation theory", *Adv. Nano Res*., **16**(4), 413-426. https://doi.org/10.12989/anr.2024.16.4.413.

Pandit, M.K., Haldar, S. and Mukhopadhyay, M. (2007), "Free vibration analysis of laminated composite rectangular plate using finite element method", *J. Reinf. Plast. Comp*., **26**, 69-80. https://doi.org/10.1177/0731684407069955.

Rabhi, M., Benrahou, K.H., Kaci, A., Houari, M.S.A., Bourada, F., Bousahla, A.A., Tounsi, A., Bedia, E.A., Mahmoud, S.R. and Tounsi, A. (2020), "A new innovative 3-unknowns HSDT for buckling and free vibration of exponentially graded sandwich plates resting on elastic foundations under various boundary conditions", *Geomech. Eng*., **22**(2), 119-132. https://doi.org/10.12989/gae.2020.22.2.119.

Rachedi, M.A., Benyoucef, S., Bouhadra, A., Bouiadjra, R.B., Sekkal, M. and Benachour, A. (2020), "Impact of the homogenization models on the thermoelastic response of FG plates on variable elastic foundation", *Geomech. Eng*., **22**(1), 65-80. https://doi.org/10.12989/gae.2020.22.1.065.

Rad, S.A.F., Hassani, B. and Karamodin, A. (2017), "Isogeometric analysis of functionally graded plates using a new quasi-3D shear deformation theory based on physical neutral surface", *Compos. B Eng*., **108**, 174-189. https://doi.org/10.1016/j.compositesb.2016.09.029.

Ramu, I. and Mohanty, S.C. (2012), "Study on free vibration analysis of rectangular plate structures using finite element method", *Procedia Eng*., **38**, 2758-2766. https://doi.org/10.1016/j.proeng.2012.06.323.

Reddy, J.N. (2000), "Analysis of functionally graded plates", *Int. J. Numer. Method. Eng*., **47**, 663-684. https://doi.org/10.1002/(SICI)1097-0207(20000110/30)47:1/3<663::AID-NME787>3.0.CO;2-8.

Reddy, J.N. (2013), "An introduction to continuum mechanics", *Cambridge university press*.

Sayyad, A.S. and Ghugal, Y.M. (2015), "On the free vibration analysis of laminated composite and sandwich plates: A review of recent literature with some numerical results", *Compos. Struct*., **129**, 177-201. https://doi.org/10.1016/j.compstruct.2015.04.007.

Shahsavari, D., Shahsavari, M., Li, L. and Karami, B. (2018), "A novel quasi-3D hyperbolic theory for free vibration of FG plates with porosities resting on Winkler/Pasternak/Kerr foundation", *Aerosp. Sci. Technol*., **72**, 134-149. https://doi.org/10.1016/j.ast.2017.11.004.

Shao, D., Hu, S., Wang, Q. and Pang, F. (2017), "Free vibration of refined higher-order shear deformation composite laminated beams with general boundary conditions", *Compos. B Eng*., **108**, 75-90. https://doi.org/10.1016/j.compositesb.2016.09.093.

Sobhy, M. (2013), "Buckling and free vibration of exponentially graded sandwich plates resting on elastic foundations under various boundary conditions", *Compos. Struct*., **99**, 76-87, https://doi.org/10.1016/j.compstruct.2012.11.018.

Tabatabaei, S.J.S. and Fattahi, A.M. (2022), "A finite element method for modal analysis of FGM plates", *Mech. Based Des. Struct*., **50**, 1111-1122, https://doi.org/10.1080/15397734.2020.1744004.

Temel, B. and Şahan, M.F. (2018), "Investigation of the efficiency of the solution of a simple mechanical model by using laplace transformation", *AJER*, **7**(10), 276-282. https://doi.org/10.47000/tjmcs.1378857.

Temel, B., Calim, F.F. and Tütüncü, N. (2004), "Quasi-static and dynamic response of viscoelastic helical rods", *J. Sound Vib*., **271**, 921-935. https://doi.org/10.1016/S0022-460X(03)00760-0.

Thai, H.T. and Choi, DH. (2012), "A refined shear deformation theory for free vibration of functionally graded plates on elastic foundation", *Compos. B Eng*., **43**, 2335-2347. https://doi.org/10.1016/j.compositesb.2011.11.062.

Turker, H.T., Cuma, Y.C. and Calim, F.F. (2023), "An efficient approach for free vibration behaviour of non-uniform and non-homogeneous helices", *IJST-T Civ. Eng.*, **47**(4), 1959-1970. https://doi.org/10.1007/s40996-023-01075-0.

Van, V.T., Tai, N.H.T. and Hung, N.N. (2021), "Static bending and free vibration analysis of functionally graded porous plates laid on elastic foundation using the meshless method", *J. Sci. Tech. Civil Eng*., **15**, 141-159. https://doi.org/10.31814/stce.nuce2021-15(2)-12.

Vel, S.S. and Batra, R.C. (2004), "Three-dimensional exact solution for the vibration of functionally graded rectangular plates", *J. Sound Vib*., **272**, 703-730, https://doi.org/10.1016/S0022-460X(03)00412-7.

Vinh, P.V. and Huy, L.Q. (2021), "Influence of variable nonlocal parameter and porosity on the free vibration behavior of functionally graded nanoplates", *Shock Vib.*, **2021**(1), 1219429. https://doi.org/10.1155/2021/1219429.

Vinh, P.V., Chinh, N.V. and Tounsi, A. (2022), "Static bending and buckling analysis of bi-directional functionally graded porous plates using an improved first-order shear deformation theory and FEM*", Eur. J. Mech.-A Solid*, **96**, 104743. https://doi.org/10.1016/j.euromechsol.2022.104743.

Xuan, H.N., Tran, L.V., Thai, C.H. and Thoi, T.N. (2012), "Analysis of functionally graded plates by an efficient finite element method with node-based strain smoothing", *Thin Walled Struct*., **54**, 1-18. https://doi.org/10.1016/j.tws.2012.01.013.

Xue, Y., Jin, G., Ma, X., Chen, H., Ye, T. and Chen, M. (2019), "Free vibration analysis of porous plates with porosity distributions in the thickness and in-plane directions using isogeometric approach", *Int. J. Mech. Sci*., **152**, 346-362. https://doi.org/10.1016/j.ijmecsci.2019.01.004.

Zhang, Y., Jin, G., Chen, M., Ye, T., Yang, C. and Yin, Y. (2020), "Free vibration and damping analysis of porous functionally graded sandwich plates with a viscoelastic core", *Compos. Struct*., **244**, 112298. https://doi.org/10.1016/j.compstruct.2020.112298.

Zhao, J., Choe, K., Xie, F., Wang, A., Shuai, C. and Wang, Q. (2018), "Three-dimensional exact solution for vibration analysis of thick functionally graded porous (FGP) rectangular plates with arbitrary boundary conditions", *Compos. B Eng*., **155**, 369-381. https://doi.org/10.1016/j.compositesb.2018.09.001.

CC

Appendix A

$$\alpha = m\pi/a,\ \beta = n\pi/b \tag{A1}$$

$$k_{11} = A_{11}\alpha^2 + A_{66}\beta^2 \tag{A2}$$

$$k_{12} = k_{21} = \alpha\beta(A_{12} + A_{66}) \tag{A3}$$

$$k_{13} = k_{31} = -B_{11}\,\alpha^3 - \alpha\beta^2(B_{12} + 2B_{66}) \tag{A4}$$

$$k_{14} = k_{41} = C_{11}\alpha^2 + C_{66}\beta^2 \tag{A5}$$

$$k_{15} = k_{51} = \alpha\beta\ (C_{12} + C_{66}) \tag{A6}$$

$$k_{22} = A_{66}\alpha^2 + A_{22}\beta^2 \tag{A7}$$

$$k_{23} = k_{32} = -B_{22}\,\beta^3 - \beta\alpha^2(B_{12} + 2B_{66}) \tag{A8}$$

$$k_{24} = k_{42} = \alpha\beta\ (C_{12} + C_{66}) \tag{A9}$$

$$k_{25} = k_{52} = C_{66}\alpha^2 + C_{22}\beta^2 \tag{A10}$$

$$k_{33} = D_{11}\alpha^4 + 2D_{12}\alpha^2\beta^2 + 4D_{66}\alpha^2\beta^2 + D_{22}\beta^4 \tag{A11}$$

$$k_{34} = k_{43} = -E_{11}\alpha^3 - \alpha\beta^2(E_{12} + 2E_{66}) \tag{A12}$$

$$k_{35} = k_{53} = -E_{22}\beta^3 - \beta\alpha^2(E_{12} + 2E_{66}) \tag{A13}$$

$$k_{44} = F_{55} + G_{11}\alpha^2 + G_{66}\beta^2 \tag{A14}$$

$$k_{45} = k_{54} = \alpha\beta\ (G_{12} + G_{66}) \tag{A15}$$

$$k_{55} = F_{44} + G_{66}\alpha^2 + G_{22}\beta^2 \tag{A16}$$

$$m_{11} = I_1 \tag{A17}$$

$$m_{12} = m_{21} = m_{15} = m_{51} = m_{24} = m_{42} = m_{45} = m_{54} = 0 \tag{A18}$$

$$m_{13} = m_{31} = -I_2\alpha \tag{A19}$$

$$m_{14} = m_{41} = I_4 \tag{A20}$$

$$m_{22} = I_1 \tag{A21}$$

$$m_{23} = m_{32} = -I_2\beta \tag{A22}$$

$$m_{25} = m_{52} = I_4 \tag{A23}$$

$$m_{33} = I_1 + I_3(\alpha^2 + \beta^2) \tag{A24}$$

$$m_{34} = m_{43} = -I_5\alpha \tag{A25}$$

$$m_{35} = m_{53} = -I_5\beta \tag{A26}$$

$$m_{44} = m_{55} = I_6 \tag{A27}$$